Theoretical annex

The influence of the magnetically induced phase condensation kinetics on the time dependence of the forward light scattering.

In the following is presented a theoretical frame for the analysis of the forward light scattering experiments, with a view to reveal the kinetics of the phase condensation process. We shall assume that the colloid comprises of three species of scatterers: MNGs assumed to be spherical and two condensed phase drops types, thin and thick, assumed to be infinitely long cylinders of randomly packed MNGs. The scattering of the MNGs and of the condensed phase drops will be treated in the Rayleigh and diffraction approximation respectively [1]. Absorption is neglected. The volume fractions of the three scatterer types, Φ_1, Φ_2 and Φ_3 respectively, obey the following conservation equation:

EqA.1. $$\begin{matrix} \Phi_1(t)+\Phi_{rps}\cdot\Phi_2(t)+\Phi_{rps}\cdot\Phi_3(t)=\Phi \\ \Phi_1(0)=\Phi,\Phi_2(0)=0,\Phi_3(0)=0 \end{matrix},$$

where Φ=1.5% is the MNG dispersion volume fraction and Φ_{rps}=0.64 is the volume fraction of randomly packed spheres [2]. It is assumed that no condensed phase drops exist in the absence of the external magnetic field.

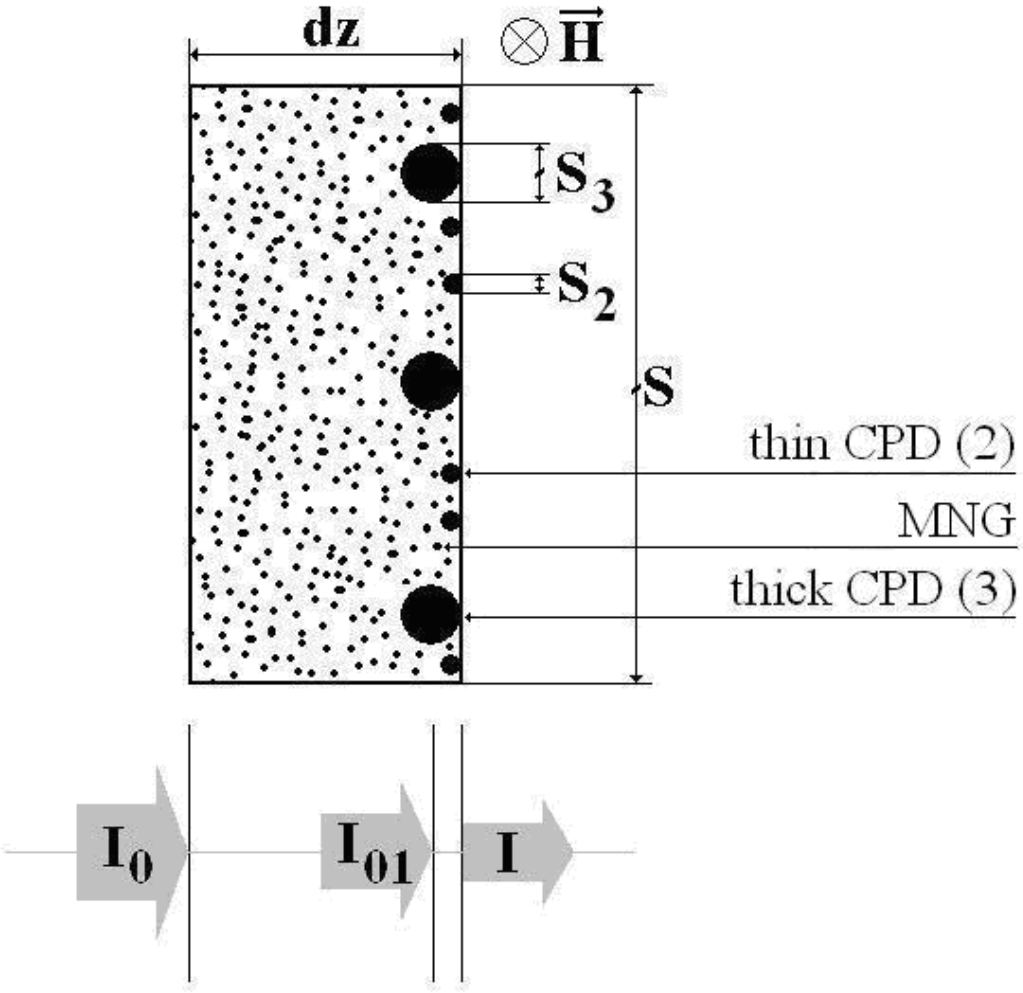

Figure A. 1 Forward scattered light through a infinitesimal sample slab.

The differential of the light scattered forward through a *dz* thickness slab of the sample is depicted in Figure A. 1. The light attenuation due to Rayleigh scattering on MNGs is [1]:

EqA.2. $I_{01} = I_0 - I_0 \cdot \Phi_1 \cdot Q_{MNG}^{sca} \cdot \frac{3}{4a_1} \cdot dz$,

where a_1 and Q_{MNG}^{sca} are the radius and the scattering efficiency of the MNGs respectively. If one assumes that *dz* is much larger than the radius of the CPDs, a_2 and a_3 respectively, the light intensity emergent from the sample in the forward direction is:

EqA.3. $I \cong (1 - df) \cdot I_{01} + df_2 \cdot I_{01} \cdot \gamma_2 + df_3 \cdot I_{01} \cdot \gamma_3$,

where *df* is the fraction that is shadowed by the CPDs from the total sample surface S. $\gamma_{2,3}$ accounts for the light scattered by the CPDs in the finite acceptance angle of the photodetector. If dn_1 and dn_2 are the number of the thin and thick CPDs in the slab, *df* is:

EqA.4. $df = df_2 + df_3 = \frac{S_{CPD2}}{S} \cdot dn_2 + \frac{S_{CPD3}}{S} \cdot dn_3$

which, in the approximation of CPDs as cylinders, becomes:

EqA.5. $df = \frac{2}{\pi}\cdot\frac{\Phi_2}{a_2}\cdot dz + \frac{2}{\pi}\cdot\frac{\Phi_3}{a_3}\cdot dz$

Using EqA.2, EqA.3 and EqA.5, neglecting the terms quadratic in *dz*, the differential intensity is:

EqA.6. $dI \cong -I\cdot\left[\Phi_1\cdot Q_{MNG}^{sca}\cdot\frac{3}{4a_1} + \Phi_2\cdot(1-\gamma_2)\cdot\frac{2}{\pi a_2} + \Phi_3\cdot(1-\gamma_3)\cdot\frac{2}{\pi a_3}\right]\cdot dz$,

which by integration leads to:

EqA.7. $I(t) = I_0\cdot e^{-\left[\Phi_1(t)\cdot Q_{MNG}^{sca}\cdot\frac{3}{4a_1} + \Phi_2(t)\cdot(1-\gamma_2)\cdot\frac{2}{\pi a_2} + \Phi_3(t)\cdot(1-\gamma_3)\cdot\frac{2}{\pi a_3}\right]\cdot h}$,

where *h* is the sample thickness. Using EqA.7 and EqA.1, the relative forward light scattering during the condensation process is:

EqA.8. $\frac{I(t)}{I(0)} = e^{-\left[(\Phi_1(t)-\Phi)\cdot Q_{MNG}^{sca}\cdot\frac{3}{4a_1} + \Phi_2(t)\cdot(1-\gamma_2)\cdot\frac{2}{\pi a_2} + \Phi_3(t)\cdot(1-\gamma_3)\cdot\frac{2}{\pi a_3}\right]\cdot h}$.

The equation above can be used to simulate the time dependence of the relative forward light scattering during the process of the magnetically induced phase condensation, provided explicit expressions for Q_{MNG}^{sca}, $\gamma_{2,3}$ and $\Phi_{1,2,3}(t)$.

The scattering efficiency of the MNGs was calculated based on the Mie theory, using *ScatLab1.2* developed by Volodynir Bazhan [3]: Q_{MNG}^{sca}=0.0067. For the calculation of Q_{MNG}^{sca} were used the TEM values of the core radius $\bar{r}_{core}$ = 27.3 nm and the pNIPA hydrated shell thickness $\bar{\delta}_{shell}$ = 13 nm. The refraction index of the pNIPA shell used was n_{pNIPA}=1.52 [4] and the refraction index of the core n_{core} was calculated using the relationship between the refractive index and the dielectric constant:

EqA.9. $\varepsilon = n^2$.

The dielectric constant of the core ε_{core} was calculated using the Maxwell-Garnett formula for a spherical region composed of spherical MNPs "immersed" in surfactant molecules [5]:

EqA.10. $\frac{\varepsilon_{core} - \varepsilon_{surf}}{\varepsilon_{core} + 2\varepsilon_{surf}} = p\cdot\frac{\varepsilon_{MNP} - \varepsilon_{surf}}{\varepsilon_{MNP} + 2\varepsilon_{surf}}$,

where $\varepsilon_{surf,\ MNP}$ are the dielectric constants of the surfactant and MNPs respectively, and *p* is the MNP volume fraction in the core. Assuming random close packing of MNPs in the core:

EqA.11. $p = \Phi_{rps}\cdot\left(\frac{\bar{r}_{MNP}}{\bar{r}_{MNP} + \bar{\delta}_s}\right)^3$,

where Φ_{rps}=0.64 is the volume fraction of randomly packed spheres [2] and from TEM investigations: $\overline{r}_{MNP}$ = 5.5 nm, $\overline{\delta}_s$ =1.1 nm. With n_{MNP}=2.2 [6] and equations EqA.9 - EqA.11, the refractive index of the core is: n_{core}=1.72.

Based on the observed evolution of the scattering patterns, one may assume that very soon after the magnetic field was switched on, very elongated CPDs were formed. Therefore, we shall approximate the CPDs as infinitely long cylinders. As a matter of fact, following Ref.[1], infinitely long cylinders are a good approximation for cylinders with aspect ratio greater than 10, whose azymuthal scattering is negligible. In the diffraction approximation, the light scattered by infinitely long cylinders in the forward direction in a θ_0 acceptance angle is [1]:

EqA.12. $$\gamma_{2,3} = \frac{\pi}{4x_{2,3}} \int_{-\theta_0}^{\theta_0} \left[\frac{1+\cos(\theta)}{\pi} \cdot \frac{x_{2,3} \cdot \sin\left(x_{2,3} \cdot \sin(\theta)\right)}{x_{2,3} \cdot \sin(\theta)} \right]^2 \cdot d\theta, \quad x_{2,3} = \frac{2\pi a_{2,3}}{\lambda}.$$

In our experiments θ_0 = 0.2°.

For the time dependence of the volume fractions $\Phi_{1,2,3}(t)$ we developed a simple phenomenological model. Taking into account the initial supersaturation degree of the MNG dispersion, i.e. the difference between the MNG volume fractions of the sample and of the equilibrium gas-like phase [7], only a part Φ_1* from the total initial MNG sample volume fraction Φ will be involved in the condensation process:

EqA.13. $$\Phi_1^*(0) = \mu \cdot \Phi .$$

where μ ($0<\mu<1$) is the parameter that controls the initial supersaturation degree of the MNG dispersion. The time dependence of the MNG volume fraction will be:

EqA.14. $$\Phi_1(t) = (1-\mu) \cdot \Phi + \Phi_1^*(t).$$

The thin CPDs are formed by the aggregation of Φ_1* MNGs, while the thick CPDs are formed by the aggregation of the thin CPDs. This process can be modeled by the second and third equations form EqA.15. The positive parameters τ_2 and τ_3 control the aggregation rate of the MNGs and thin CPDs, i.e. having, by analogy to the chemical kinetics, the meaning of ‘reaction” rates for the formation of the thin and thick CPDs respectively. Due to the viscous drag, the diffusion coefficient is much larger for thin the CPDs than for the MNGs, whence $\tau_2>\tau_3$. Using the differential of EqA.1, $\Phi_{1*,2,3}(t)$ obey the following set of ordinary differential equations:

$$\frac{d\Phi_1^*(t)}{dt} = -\Phi_{rps}\cdot\tau_2\cdot\Phi_1^*(t) - \Phi_{rps}\cdot\tau_3\cdot\Phi_2(t) + \Phi_{rps}\cdot\tau_3\cdot\Phi_3(t)$$

EqA.15. $$\frac{d\Phi_2(t)}{dt} = \tau_2\cdot\Phi_1^*(t) - \tau_3\cdot\Phi_3(t) \quad ,$$

$$\frac{d\Phi_3(t)}{dt} = \tau_3\cdot\Phi_2(t)$$

with initial conditions:

EqA.16. $$\Phi_1^*(0) = \mu\cdot\Phi,\ \Phi_2(0) = 0,\ \Phi_3(0) = 0\,.$$

Together with Φ, the volume fraction of the MNG dispersion, μ, τ_2 and τ_3 are constant parameters of the model. The equations EqA.15 and EqA.16, together with EqA.14, admit analytical solutions for $\Phi_{1,2,3}(t)$. The mathematical expressions of the solutions are too long and cumbersome to be worth printing. However, due to the presence of the factor $\left(\sqrt{1-4\frac{\tau_3}{\tau_2\Phi_{rps}}-4\left(\frac{\tau_3}{\tau_2\Phi_{rps}}\right)^2}\cdot t\right)$ in the exponential terms from all $\Phi_{1,2,3}(t)$ solutions, depending upon the relationship between τ_2 and τ_3, the possibility is that the condensation process may enter into a dynamical oscillatory regime. Thus, if $\tau_3/(\tau_2\Phi_{rps})<1.2$, $\Phi_1(t)$ and $\Phi_3(t)$ are monotonous real functions of time, the former decreasing and the later increasing, while if $\tau_3/(\tau_2\Phi_{rps})>1.2$, $\Phi_{1,2,3}(t)$ are oscillating complex functions of time.

In Figure A. 2 is presented a plot of the three functions $\Phi_{1,2,3}(t)$, for $\Phi = \Phi_{hyd} = 1.5\%$, $\mu=2/3$ and two physically meaningful sets of rate constants: $\{\tau_2=0.02\ s^{-1},\ \tau_3=0.0001\ s^{-1}\}$ and $\{\tau_2=0.02\ s^{-1},\ \tau_3=0.0002\ s^{-1}\}$ respectively. Other parameter combinations may lead to physically meaningless situations where one or more of the volume fraction functions become negative. At the beginning, the volume fraction of the thin CPDs ($\Phi_2(t)$) sharply grows on the expense of the MNG volume fraction ($\Phi_1(t)$). The thick CPDs volume fraction ($\Phi_3(t)$) growth is slower, but eventually leads to a decay of the thin CPDs volume fraction. The growth rate of the thick CPDs volume fraction increases with increasing τ_3 / τ_2 ratio. Qualitatively, $\Phi_{1,2,3}(t)$ provide a good mathematical description of the optical microscopy observations on the process of magnetically induced phase condensation.

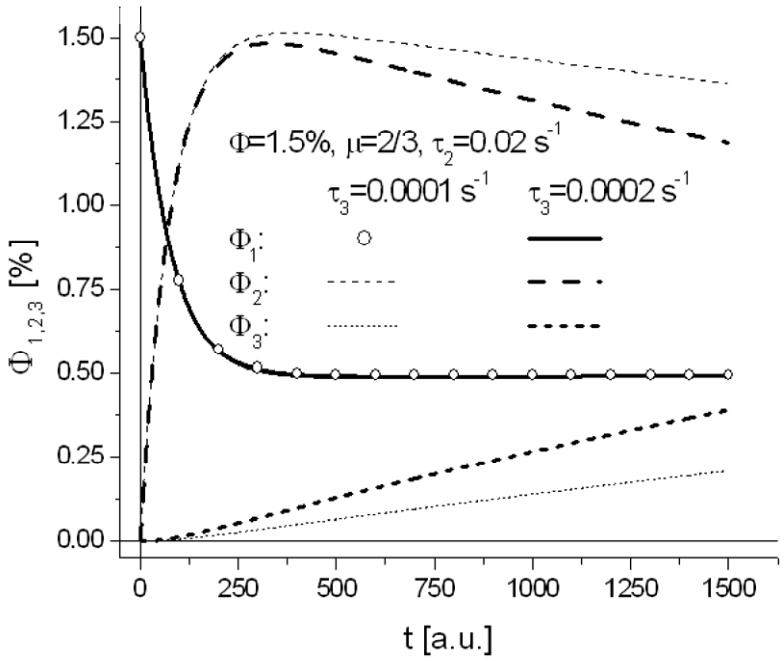

Figure A. 2 The time dependence of the colloid composition for $\tau_3 = 0.0001\ s^{-1}$ and $\tau_3 = 0.0002\ s^{-1}$ ($\Phi = 1.5\%$, $\mu=2/3$, $\tau_2=0.02\ s^{-1}$).

All the mathematical apparatus is now ready to simulate the time dependence of the relative forward light scattering during the process of the magnetically induced phase condensation. The simulation data presented in Figure A. 3 a), b) and c) summarizes the influence on the relative forward scattering kinetics of the three constant parameters of the model: the growth rates of the thin (τ_2) and thick (τ_3) CPDs, and the supersaturation degree (μ) of the MNG dispersion. In the inset of Figure A. 3 a) is presented the dependence of the relative forward scattering on the cylinder radius in the hypothesis that, after a long enough field exposure, the entire population of MNGs will condense into CPDs with radius *a*. The monotonous increase of the relative forward scattering with increasing cylinder radius is a well known scattering property of particles comparable or larger than the wavelength [1]. Therefore, the fact that the relative forward scattering may decay during the condensation process is the result of the competition between the scattering properties of the different types of scatterers (MNGs, thin and thick CPDs) and their relative concentrations. Based on the optical microscopy observations, the radius of the CPDs used in simulations were: $a_2 = 0.5$ μm and $a_3 = 2$ μm.

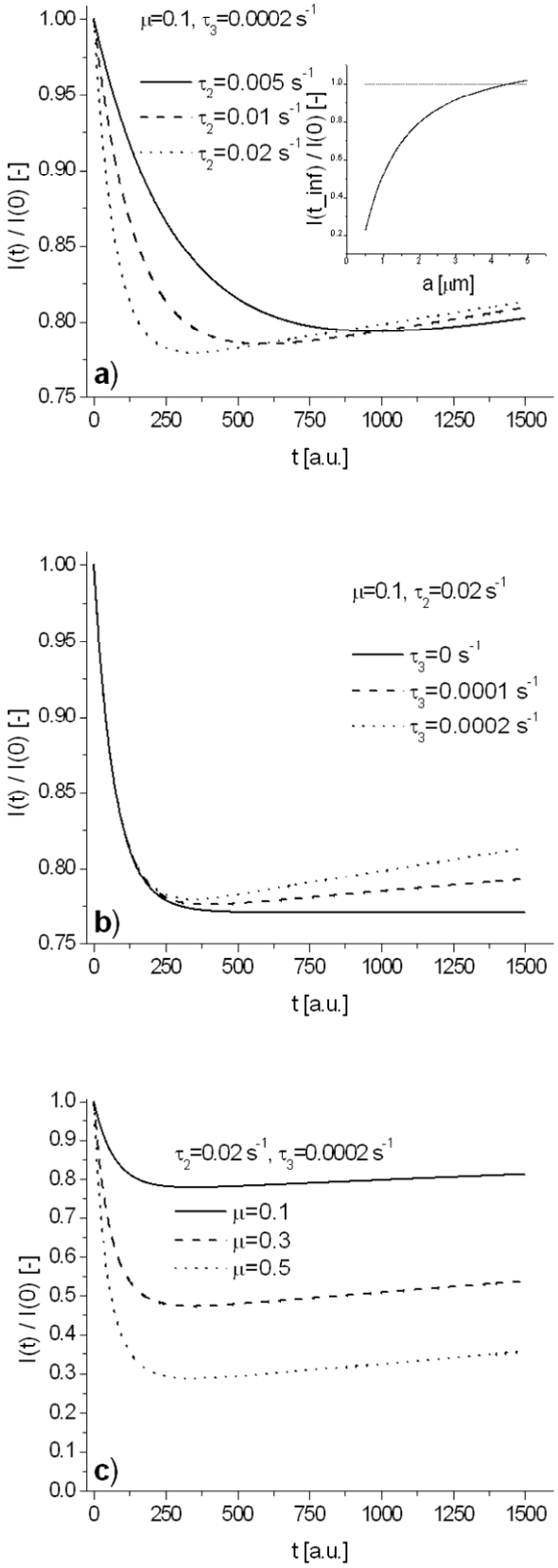

Figure A. 3 The influence of the model parameters a) τ_2, b) τ_3, and c) μ, on the time dependence of the relative forward scattering.

The higher the rate of the thin CPDs formation, the steeper is the initial decrease of the relative forward scattering (Figure A. 3 a)). Should no thick CPDs are being formed (τ_3=0), the relative forward scattering will remain constant after the thin CPDs formation is saturated (Figure A. 3 b)). However, the formation of thick CPDs leads to a regime of relative forward scattering increase, with a rate proportional to τ_3 (Figure A. 3 b)). The absolute diminishing of the relative forward scattering during the condensation process is increasing with the degree of the initial magnetically induced supersaturation of the MNG dispersion (Figure A. 3 c)).

From the comparison of the data in Figure A. 2 and Figure A. 3 one can observe that the minimum of the relative forward scattered light is reached when Φ_1*=0, i.e. when the magnetically induced supersaturation of the sample vanishes. Therefore, the minimum value of the relative forward scattered light is mainly determined by the initial supersaturation degree μ. The value of the initial supersaturation degree can be obtained by equating the solution of equations EqA.15 and EqA.16 with the measured minimum value of the relative forward scattered light. The instantaneous supersaturation however, as shown in Figure A. 3 a), is mainly and strongly dependent by the aggregation rate of the MNGs (τ_2).

References

1. C.F. Bohren and D.R. Huffman, *Absorption and Scattering of Light by Small Particles*, John Wiley & Sons, 1983.
2. S. Torquato, F.H. Stillinger, *Rev.Mod.Phys.*, 2010, **82**, 2633.
3. http://www.scatlab.org/index.html
4. M. Reufer, P. Díaz-Leyva, I. Linch, P. Scheffold, *Eur.Phys.J. E,* 2009, **28**, 165.
5. S. Berthier, *Optique des milieux composites*, POLYTECHNICA, 1983.
6. M. Xu, P.J. Ridler, *J. Appl. Phys.*, 1997, **82**, 326.
7. A.Yu. Zubarev, A.O. Ivanov, *Physica A*, 1998, **251**, 332.

Color versions of Fig. 6 and Fig. 7 from the paper

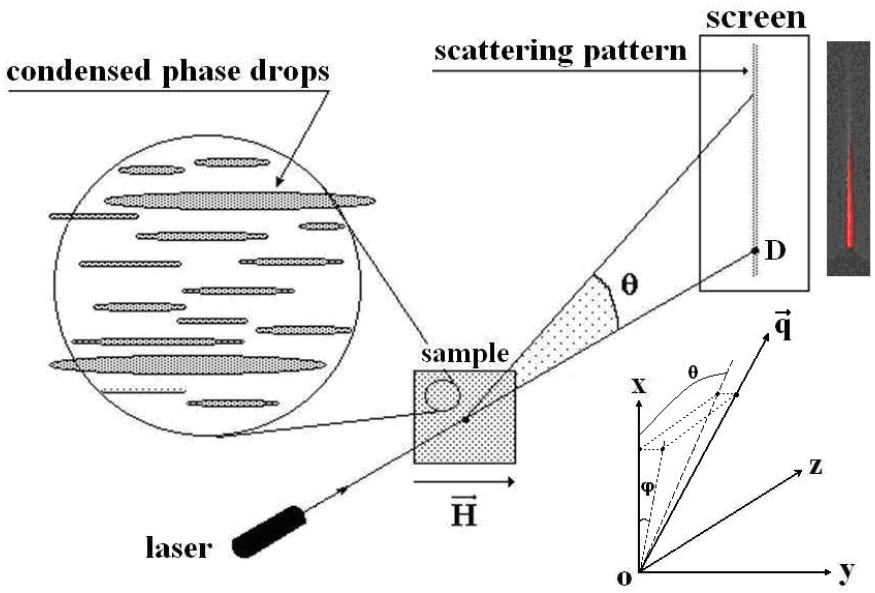

Fig. 6 Laser beam scattering by condensed phase drops.

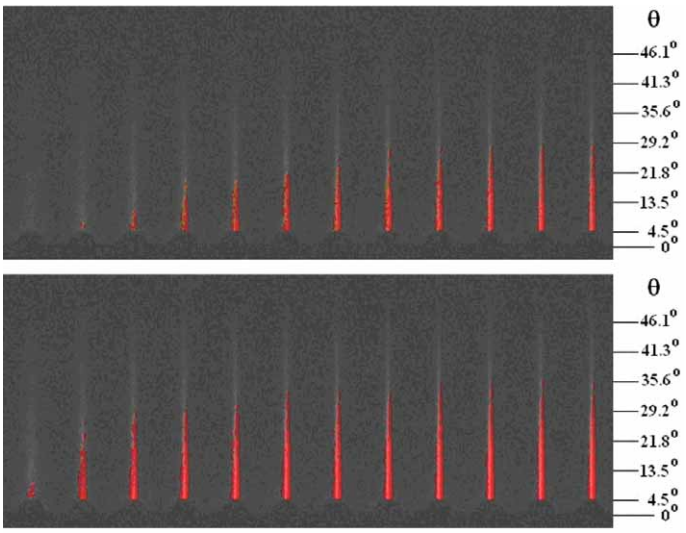

Fig. 7 Light scattering patterns at 5 seconds successive intervals after field onset for H=20 kA/m (top)and for H=40 kA/m (bottom) (the sample temperature was 30°C).